Pilot Insertion Rate for SC-FDE Systems Employing Subspace-Based Channel Estimation

Shiva Gholami-Boroujeny[1], Adel O. Dahmane[2],*Member, IEEE*, and Claude D'Amours[1],*Member, IEEE*
[1] School of Electrical Engineering and Computer Science
University of Ottawa,
Ottawa, Canada
[2] Département de génie électrique et génie informatique
Université du Québec à Trois Rivières,
Trois Rivières, Canada

***Abstract*—Blind or semi-blind channel estimation techniques, such as subspace decomposition, often use second order statistics which can provide channel estimates that are multiplied by an unknown complex constant, known as the ambiguity. Determination of this ambiguity can be achieved by the insertion of a small number of pilot symbols within a data block. The goal of this paper is to investigate the bit error rate performance of single carrier frequency domain equalization (SC-FDE) based transmissions using different pilot insertion rates, with the goal of determining the ambiguity without sacrificing spectral efficiency. Using Monte Carlo simulation, our results show, for the conditions presented in this paper, the insertion of 4 pilot symbols per 64 symbol block (or a ratio of 1 pilot per 15 information symbols) achieves a BER of 10^{-3} with a power loss of 1dB or 1.5 dB (depending on the channel order) compared to a system with perfect ambiguity resolution.**

***Index Terms*—Channel Estimation, Wireless Communication, Blind Equalizers, Adaptive Equalizers**

I. Introduction

SINGLE carrier frequency division multiple access (SC-FDMA), a multiple user version of single carrier frequency domain equalization (SC-FDE), is proposed for 4G uplinks due to the high peak-to-average power ratio (PAR) of orthogonal frequency division multiplexed (OFDM) systems [1, 2]. In OFDM, subcarrier channel estimate errors affect only the symbol carried on that particular subcarrier. One drawback of SC-FDE based systems is that a channel estimation error on any subcarrier affects all symbols in a frame; therefore reliable channel estimation techniques are needed.

Prior work on channel estimation techniques for SC-FDMA and SC-FDE systems presented in the literature focuses on using pilots in either the time or the frequency domain to estimate the frequency response of the channel [3, 4]. In the uplink of 4G systems, the current state of the art is to use pilots for channel estimation. As described in [5], the channel gains are estimated by periodically transmitting a frame made up entirely of pilots for the purpose of channel estimation. However, in doing so, the spectral efficiency is reduced because the transmission of pilot symbols increases the rate of symbols transmitted over the channel, thus increasing the bandwidth of the transmission, without a corresponding increase in the amount of information-bearing symbols.

To perform channel estimation without a corresponding loss in spectral efficiency, one can use blind or semi-blind techniques which perform channel estimation using data that is not known to the receiver. By reducing the dependency on pilot data, the overall spectral efficiency is increased. Due to their ability to train using unknown symbols rather than pilots, blind techniques are considered more attractive than their pilot-trained counterparts in terms of improved spectral efficiency. However, they tend to be more computationally complex, which may discourage the use of these techniques.

Subspace decomposition is one of a number of second order statistical methods that can be used for blind or semi-blind channel estimation. When multiple receive antennas are used, the autocorrelation of the observation can be used to determine the channel impulse responses between all transmit-receive antenna pairs, up to a constant [6- 9]. Determination of this constant, referred to as the ambiguity, usually requires the insertion of a small number of known data points, thus resulting in a semi-blind approach. However, in order for the subspace decomposition technique to yield better spectral efficiencies than typical pilot based approaches, the pilot insertion rate to correct the ambiguity must be comparatively small. In this paper, we consider pilot insertion rates for ambiguity resolution to determine an acceptable tradeoff between bit error rate (BER) and channel estimation accuracy measured by normalized mean square error versus pilot insertion rate.

The rest of the paper is organized as follows. Section II describes the SC-FDE system model. In Section III, subspace decomposition is summarized. Section IV details the proposed ambiguity resolution for subspace decomposition approach in SC-FDE systems. In Section V, the performance results are determined by Monte Carlo simulations. In Section VI, we present our conclusions.

978-1-4799-8088-8/15/$31.00 ©2015 IEEE

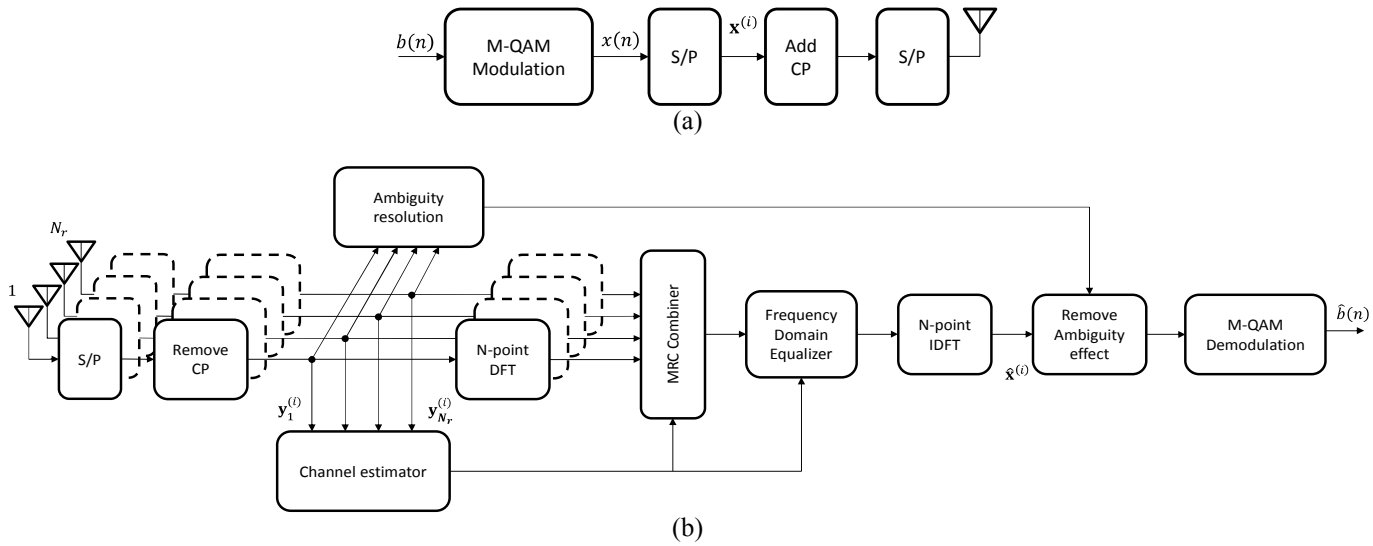

Fig. 1. Block diagram of the SC-FDE system (a) Transmitter and (b) multi-antenna receiver with channel estimation, frequency domain equalizer and ambiguity resolution

II. SC-FDE SYSTEM

In Fig. 1, the SC-FDE system with one transmitting antenna and N_r receiving antennas $(N_r > 1)$ is shown. Bit streams are grouped in blocks of N_b bits where the i^{th} block is:

$$\mathbf{b}^{(i)} = \left[b^{(i)}(0)b^{(i)}(1) \dots b^{(i)}(N_b - 1)\right]^T \quad (1)$$

where T is the transpose operator.

Each block of bits $\mathbf{b}^{(i)}$ is modulated using M-ary quadrature amplitude modulation (M-QAM) by converting each M_b bits into one symbol. Therefore, a block of N symbols is formed and given by

$$\mathbf{x}^{(i)} = \left[x^{(i)}(0)x^{(i)}(1) \dots x^{(i)}(N-1)\right]^T \quad (2)$$

where $N = N_b/M_b$.

A cyclic prefix (CP) is added in each block to ensure circular convolution with the wireless channel impulse responses in the time domain. In the case of the SC-FDE system considered in this study, N_r channels are modeled as discrete time impulse responses.

For the i^{th} message block, channels are given by

$$h_l^{(i)}(n) = \sum_{k=0}^{M} h_{l,k}^{(i)}\delta(n-k),\ l = 1, \dots, N_r \quad (3)$$

where M is the channel order and $h_{l,k}^{(i)}$ is the complex gain of the kth resolvable path on the lth channel. Frequency selective fading is assumed with Rayleigh distribution. The coefficients $h_{l,k}^{(i)}$ are therefore independent circularly symmetric complex Gaussian random variables. We also assume that these channel coefficients are constant for the duration of a message block.

At the receiver side, the CP is removed. After that, serial to parallel conversion is performed; followed by an N-point discrete Fourier transform (DFT). The N_r DFT outputs are combined using maximal ratio combining (MRC) and frequency domain equalization (FDE) is performed in order to remove the wireless channel effects. From the mathematical development provided in [10], equations (4) to (10) describe the outputs of the major blocks in Fig. 1 at the receiver side and especially the estimate of the DFT of the transmitted symbols in (10).

$$\mathbf{y}_l^{(i)} = \left[y_l^{(i)}(0)y_l^{(i)}(1) \dots y_l^{(i)}(N-1)\right]^T \quad (4)$$

$$\mathbf{y}_l^{(i)} = \mathbf{x}^{(i)} \circledast \mathbf{h}_l^{(i)} + \mathbf{z}_l^{(i)} \quad (5)$$

$$\mathbf{h}_l^{(i)} = \left[h_{l,0}^{(i)}h_{l,1}^{(i)} \dots h_{l,M}^{(i)}\right]^T \quad (6)$$

$$\mathbf{z}_l^{(i)} = \left[z_l^{(i)}(0)z_l^{(i)}(1) \dots z_l^{(i)}(N-1)\right]^T \quad (7)$$

$$Y_l^{(i)}(m) = X^{(i)}(m)H_l^{(i)}(m) + Z_l^{(i)}(m) \quad (8)$$

$$Y^{(i)}(m) = \sum_{l=1}^{N_r} Y_l^{(i)}(m)\hat{H}_l^{(i)*}(m) \quad (9)$$

$$\hat{X}^{(i)}(m) = \frac{Y^{(i)}(m)}{\sum_{l=1}^{N_r}\left|\hat{H}_l^{(i)}(m)\right|^2 + \sigma_z^2} \quad (10)$$

IN the previous equations, $\circledast$ denotes circular convolution due to CP; * denotes the conjugate; $\boldsymbol{H}_l^{(i)} = \left[H_l^{(i)}(0) \dots H_l^{(i)}(N-1)\right]$, The vectors $\mathbf{Y}_l(i) = Y_l(0) \dots Y_l(N-1)$, and $\mathbf{Z}_l(i) = Z_l(i)0 \dots Z_l(i)N-1$ are the N-point DFTs of $\mathbf{x}(i)$, $\mathbf{h}_l(i)$, $\mathbf{y}_l(i)$, and $\mathbf{z}_l^{(i)}$ respectively; and $\mathbf{z}_l^{(i)}$ represent the additive white noise with variance σ_z^2.

As previously mentioned, (10) is the estimate the DFT of transmitted symbols using minimum mean square error (MMSE) equalization. In the absence of an estimate of the noise level, it is possible to use the zero forcing. In this case, equation (10) simplifies to

$$\hat{X}^{(i)}(m) = \frac{Y^{(i)}(m)}{\sum_{l=1}^{N_r}\left|\hat{H}_l^{(i)}(m)\right|^2} \quad (11)$$

To perform MRC and FDE, channel estimation operation is mandatory. Blind channel estimation techniques allow spectral efficiency while providing good results up to a constant known as the ambiguity. In the next section, we will introduce this ambiguity along with its resolution.

III. SUBSPACE DECOMPOSITION

Let $L < N$ denote the size of the data vectors used at each antenna for the purpose of channel estimation. Considering the current as well as previous $L-1$ outputs of each antenna after the CP has been removed, we define the corresponding data vector as

$$\mathbf{y}_l^{(i)}(n) = \left[y_l^{(i)}(n)\ y_l^{(i)}(n-1)\ \ldots\ y_l^{(i)}(n-L+1)\right]^T \quad (12)$$

where $L-1 \le n \le N-1$ (all observations occur in the same data block) and we also define the complete $N_r L \times 1$ data vector as

$$\mathbf{y}^{(i)}(n) = \left[\ \mathbf{y}_1^{(i)}(n)^T\ \mathbf{y}_2^{(i)}(n)^T\ \ldots\ \mathbf{y}_{N_r}^{(i)}(n)^T\right]^T \quad (13)$$

Assuming the channel variations are sufficiently slow so that the channel can be considered static over the duration of the data block, then we can express (11) as

$$\mathbf{y}^{(i)}(n) = \mathcal{H}^{(i)}\mathbf{x}^{(i)}(n) + \mathbf{z}^{(i)}(n) = \left[\mathcal{H}_1^{(i)^T}\ \mathcal{H}_2^{(i)^T}\ \ldots\ \mathcal{H}_{N_r}^{(i)^T}\right]^T \mathbf{x}^{(i)}(n) + \mathbf{z}^{(i)}(n) \quad (14)$$

where

$$\mathcal{H}_l^{(i)} = \begin{bmatrix} h_{l,0}^{(i)} & h_{l,1}^{(i)} & \ldots & h_{l,M}^{(i)} & 0 & \ldots & 0 \\ 0 & h_{l,0}^{(i)} & h_{l,1}^{(i)} & \ldots & h_{l,M}^{(i)} & \ldots & 0 \\ \vdots & \vdots & \ddots & \vdots & \vdots & \ddots & \vdots \\ 0 & 0 & \ldots & h_{l,0}^{(i)} & h_{l,1}^{(i)} & \ldots & h_{l,M}^{(i)} \end{bmatrix} \quad (15)$$

is the $L \times (L+M)$ channel matrix for the lth channel, $\mathbf{x}_l^{(i)}(n) = \left[x^{(i)}(n)\ x^{(i)}(n-1)\ \ldots\ x^{(i)}(n-M-L+1)\right]^T$ is the $(L+M)\times 1$ channel input vector, $\mathbf{z}^{(i)}(n) = \left[\mathbf{z}_1^{(i)}(n)^T\ \mathbf{z}_2^{(i)}(n)^T\ \ldots\ \mathbf{z}_{N_r}^{(i)}(n)^T\right]^T$ and

$$\mathbf{z}_l^{(i)}(n) = \left[\mathbf{z}_l^{(i)}(n)\ \mathbf{z}_l^{(i)}(n-1)\ \ldots\ \mathbf{z}_l^{(i)}(n-L+1)\right]^T \quad (16)$$

Assuming that the transmitted data is temporally independent with zero mean and unit variance, then $E\left[\mathbf{x}^{(i)}(n)\mathbf{x}^{(i)H}(n)\right] = \mathbf{I}_{N_r(M+L)}$, which is an identity matrix of order $N_r(M+L)$. We define the output correlation matrix of $\mathbf{y}^{(i)}(n)$ as $\mathbf{R}_y^{(i)} = E\left[\mathbf{y}^{(i)}(n)\mathbf{y}^{(i)}(n)^H\right]$.

The $N_r L \times N_r L$ correlation matrix $\mathbf{R}_y^{(i)}$ can be expressed in terms of its eigenvalues and associated orthonormalized eigenvectors as:

$$\mathbf{R}_y^{(i)} = \sum_{k=0}^{N_r L-1} \lambda_k\, \mathbf{q}_k \mathbf{q}_k^H \quad (17)$$

where the eigenvalues are arranged in decreasing order, i.e. $\lambda_0 \ge \lambda_1 \ge \cdots \ge \lambda_{N_r L-1}$. Since $\mathbf{R}_y^{(i)}$ has rank $N_r L$ and the signal part has rank $L+M$ then we can divide these eigenvalues into two groups [11]:

1. $\lambda_k > \sigma_Z^2,\ 0 \le k \le M+L-1$
2. $\lambda_k = \sigma_Z^2,\ M+L \le k \le N_r L-1.$

The space spanned by the eigenvectors of $\mathbf{R}_y^{(i)}$ can then be separated into two subspaces: the signal subspace is spanned by the eigenvectors associated to the first group while the noise subspace is spanned by those associated to the second group. The ability to separate the eigenvectors into two subspaces implies that M is known.

Let $\mathbf{g}_k = \mathbf{q}_{M+L+k}$ for $0 \le k \le N_r L - M - L - 1$ be the set of eigenvectors of $\mathbf{R}_y^{(i)}$ which span the noise subspace. It is shown in [11] that:

$$\mathcal{H}^{(i)H}\mathbf{g}_k = \mathbf{0} \quad (18)$$

which means that the columns of the unknown multichannel matrix are orthogonal to the noise subspace. Equivalently, we can rewrite (18) as:

$$\mathbf{g}_k^H \mathcal{H}^{(i)}\mathcal{H}^{(i)H}\mathbf{g}_k = 0 \quad (19)$$

Since $\mathcal{H}^{(i)}$ has a partitioned structure as shown in (14), it is natural to assume a corresponding structure for the $N_r \times 1$ eigenvector, therefore $\mathbf{g}_k = \left[\mathbf{g}_k^{(1)T}\ \mathbf{g}_k^{(2)T}\ \ldots\ \mathbf{g}_k^{(N_r)T}\right]^T$ where $\mathbf{g}_k^{(l)} = \left[g_{k,0}^{(l)}\ g_{k,1}^{(l)}\ \ldots\ g_{k,L-1}^{(l)}\right]^T$. It is shown in [11] that:

$$g_k^H \mathcal{H}^{(i)}\mathcal{H}^{(i)H} g_k = h^{(i)H}\mathcal{G}_k\mathcal{G}_k^H h^{(i)} = 0 \quad (20)$$

where

$$\mathcal{G}_k = \left[\mathbf{G}_k^{(1)T}\ \mathbf{G}_k^{(2)T}\ \ldots\ \mathbf{G}_k^{(N_r)T}\right]^T \quad (21)$$

$$\mathbf{G}_k^{(l)} = \begin{bmatrix} g_{k,0}^{(l)} & \ldots & g_{k,L-1}^{(l)} & 0 & \ldots & 0 \\ 0 & g_{k,0}^{(l)} & \ldots & g_{k,L-1}^{(l)} & \ldots & 0 \\ \vdots & \ddots & \vdots & \vdots & \ddots & \vdots \\ 0 & 0 & \ldots & g_{k,0}^{(l)} & \ldots & g_{k,L-1}^{(l)} \end{bmatrix} \quad (22)$$

and

$$\mathbf{h}^{(i)} = \left[\ \mathbf{h}_1^{(i)T}\ \mathbf{h}_2^{(i)T}\ \ldots \mathbf{h}_{N_r}^{(i)T}\ \right]^T \quad (23)$$

is an $N_r(M+1)\times 1$ channel gain vector, $\mathbf{h}_l^{(i)}$ being the desired channel gain vector in (6).

In practice, we need to estimate $\mathbf{R}_y^{(i)}$ and its corresponding eigenvectors $\mathbf{g}_k^{(i)}$ by averaging over time as is done in [10]. In this work we consider exponential averaging with forgetting factor μ yielding $\hat{R}_y^{(i)}$.

Performing the eigenvector decomposition of $\hat{R}_y^{(i)}$ yields the set of eigenvectors $\{\mathbf{v}_k\}$ and associated eigenvalues $\{\rho_k\}$ for $k = 0, 1, \ldots, N_r L - 1$. We approximate the eigenvectors of the noise subspace, $\mathbf{g}_k$ by selecting the eigenvectors that correspond to the $(N_r-1)L-M$ smallest eigenvalues of $\hat{R}_y^{(i)}$. Assuming that $\rho_0 \ge \rho_1 \ge \cdots \ge \rho_{N_r L-1}$ then

$$\hat{\mathrm{g}}_k = \mathbf{v}_{M+L+k},\ 0 \le k \le (N_r-1)L - M - 1 \quad (24)$$

By replacing $\mathbf{g}_k$ by $\hat{\mathrm{g}}_k$ in (19), and (22) we obtain an estimate for $\mathcal{G}_k$ which we denote as $\hat{\mathcal{G}}_k$. Then, based on (20), we define:

$$Q = \sum_{k=0}^{(N_r-1)L-M-1} \hat{\mathcal{G}}_k \hat{\mathcal{G}}_k^{\mathrm{H}} \quad (25)$$

and consider a cost function $\mathcal{E}(\mathbf{h}) = \mathbf{h}^H Q \mathbf{h}$. Let $\mathbf{h} = \hat{\mathrm{h}}^{(i)}$ be the vector that minimizes this cost function subject to $\left\|\hat{\mathrm{h}}^{(i)}\right\| = 1$. Then the estimate of the N_r channel impulse responses is $\hat{\mathrm{h}}^{(i)}$ and is given by

$$\hat{\mathbf{h}}^{(i)} = c(\mathbf{h}^{(i)} + \mathbf{h}_e^{(i)}) \quad (26)$$

where $\mathbf{h}^{(i)}$ is given by (23), $\mathbf{h}_e^{(i)}$ is the estimation error and c is an unknown complex multiplicative constant defined as the ambiguity [11].

IV. AMBIGUITY RESOLUTION

The role of channel estimation technique is to obtain a close estimate (23) given (26). We proceed by assuming that $\mathbf{h}_e^{(i)} = 0$. In this case, equation (26) becomes

$$\hat{\mathbf{h}}^{(i)} = c\mathbf{h}^{(i)} \quad (27)$$

From (27) and the fact that DFT operation is linear, $\hat{H}_l^{(i)}$ in (15) becomes

$$\hat{H}_l^{(i)} = cH_l^{(i)} \quad (28)$$

Using (28), then (11) becomes

$$\hat{X}^{(i)}(m) = \frac{c^* \sum_{l=1}^{Nr} Y_l^{(i)}(m) H_l^{(i)*}(m)}{|c|^2 \sum_{l=1}^{Nr} \left|H_l^{(i)}(m)\right|^2} \quad (29)$$

and (29) can be further simplified to

$$\hat{X}^{(i)}(m) = \frac{c^*}{|c|^2} X^{(i)}(m) \quad (30)$$

Or equivalently

$$X^{(i)}(m) = c\hat{X}^{(i)}(m) \quad (31)$$

Therefore, to resolve this ambiguity and without a large sacrifice in spectral efficiency, we can insert a small number of pilot symbols within a data block. We denote N_p as the number of pilot symbols that can be interleaved in each symbol block. Consider

$$\mathbf{x}_p^{(i)} = \left[x(p_1) \ \ldots \ x(p_{Np})\right] \quad (32)$$

which are the known symbols transmitted as the pilot vector where $p_n(p_n = 1, \ldots, N_p)$ is the n^{th} pilot symbol within the symbol block, and let

$$\hat{\boldsymbol{x}}_p^{(i)} = \left[\hat{x}_p^{(i)}(1) \ \ldots \ \hat{x}_p^{(i)}(N_p)\right] \quad (33)$$

be the corresponding estimated symbols at the receiver.

From (31) and the linearity of the DFT, we have

$$\mathbf{x}_p^{(i)} = c\hat{\boldsymbol{x}}_p^{(i)} \quad (34)$$

The ambiguity can be determined easily from (34)

$$c = \frac{\hat{\mathbf{x}}_p^{(i)H} \mathbf{x}_p^{(i)}}{\hat{\mathbf{x}}_p^{(i)H} \hat{\mathbf{x}}_p^{(i)}} \quad (35)$$

The number of pilot symbols will be determined by Monte Carlo simulation. The results will be presented in the next section.

V. SIMULATION RESULTS

The SC-FDE system presented in Fig. 1 has been simulated using parameters of Table 1. Quasi-static frequency selective Rayleigh fading channels with equal strength paths have been considered. The relationship between two consecutive blocks of channel coefficients is produced using a first order autoregressive model

$$E\left[\mathbf{h}^{(i)H}\mathbf{h}^{(i+1)}\right] / \left(\left\|\mathbf{h}^{(i)}\right\| \left\|\mathbf{h}^{(i+1)}\right\|\right) = J_0(2\pi B_d T) \quad (36)$$

where B_d is the Doppler spread and T is the data block interval. The exponential window averaging is performed using the value of μ in Table 1 [10]. We assume that channel order determination is performed perfectly.

To evaluate the performance of the ambiguity resolution and the impact of pilot insertion, two metrics have been used:

- The first one is the NMSE (normalized mean square error) between perfect and estimated channel gains in the frequency domain

$$NMSE = \frac{E\left[\left|\hat{H}_l^{(i)}(m) - H_l^{(i)}(m)\right|^2\right]}{E\left[\left|H_l^{(i)}(m)\right|^2\right]} \quad (37)$$

- The second metric is the BER (Bit Error Rate) of the system described in this study relative to the signal to noise ratio E_b/N_o; where E_b is the energy per bit and N_o is the single sided noise spectral density.

Results are presented for different number of pilot symbols (from 1 to 6) and for two different channel orders (4 and 7). Simulation results are presented by averaging on 30000 blocks of symbols.

Fig. 2 shows the NMSE of the subspace-based channel estimation when channel order $M = 4$. We compare the performance of the proposed ambiguity resolution when different number of pilot symbols are used to the perfect ambiguity resolution estimation. The latter is used as a reference curve. As expected, as the number of pilot symbols increase, the performance the ambiguity resolution improves. At 4 pilot symbols or above, we have tiny improvements.

In Fig. 3, using the same simulation conditions as for Fig.2, we have BER performances using different number of pilot symbols. As in previous figure, we show the perfect ambiguity estimation as a reference curve. We notice the same performance tendency regarding the number of pilot symbols insertion. For example, at BER of 10^{-3}, we observe a loss of approximately 1.5dB in terms of E_b/N_o when 4 pilot symbols are used. This loss almost doubles when two pilot symbols are used. With one pilot symbol, the system is not able to reach this BER. We notice also that above 4 pilot symbols, a gain of only a fraction of dBs is obtained when compared to perfect ambiguity estimation.

TABLE I Simulation parameters

Symbol	Quantity
M_b	16-QAM modulation
N_r	4
N	64
CP	6 or 9
B_dT	0.025
μ	0.4
N_p	1, 2, 3, 4, 5 or 6
M	4 or 7

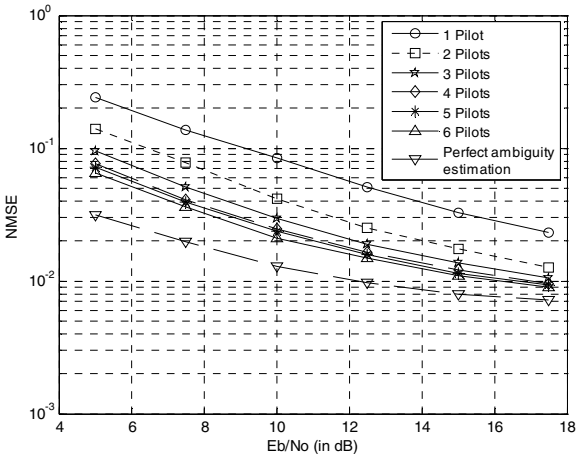

Fig. 2. NMSE of subspace-based channel estimates as a function of E_b/N_o for different numbers of pilot symbols used for ambiguity resolution with channel order = 4

In this study, we have run different simulations in order to study the effect of channel ambiguity resolution depending on the pilot locations. As expected, due to the channel behavior, a distributed pilot insertion provides the best performance. The performance presented in case of 4 pilot symbols insertion for example are obtained when the pilot symbols are inserted in $n_1 = 1$, $n_2 = 22$, $n_3 = 43$, and $n_4 = 64$ inside each symbol block.

In Fig.4 and Fig. 5, we have run the same set of simulations for channel order $M = 7$. Since a higher channel order is used, results obtained in Fig. 4 with perfect ambiguity estimation are worse than those of Fig. 2. From Fig. 4, we observe also that NMSE improves as the number of pilot symbols increases. But in this case, slight improvements are observed with a number of pilot symbols equal to 4 or above compared to the perfect ambiguity estimation. The last observation is also noticed in Fig. 5. Indeed, with 4 pilot symbols, a loss of 1dB is observed at BER of 10^{-3} when compared to perfect ambiguity estimation case. In this case also, only a fraction of performance loss is observed compared to 6 pilot symbols insertion case. It is worth mentioning that best results have been obtained, as in the previous case, when the pilot symbols are at positions $n_1 = 1$, $n_2 = 22$, $n_3 = 43$, and $n_4 = 64$ inside each symbol block.

VI. Conclusion

In this paper, we addressed the problem of pilot insertion rate for subspace-based channel estimation in SC-FDE systems. We show that using only a small number of pilot symbols for ambiguity resolution is enough to reach accurate channel estimates. For a system employing 4 receive antennas, 16QAM modulation and 64 symbol FFT blocks which uses 4 pilot symbols for ambiguity resolution and operates in a slowly fading 5 tap channel, we show that a BER of 10^{-3} can be achieved with a power loss of roughly 1.5 dB compared to a system with perfect ambiguity estimates. Under the same aforementioned conditions, a power loss of 1.0 dB can be achieved with the same number of pilot symbols for a system that operates in a slowly fading 8 tap channel.

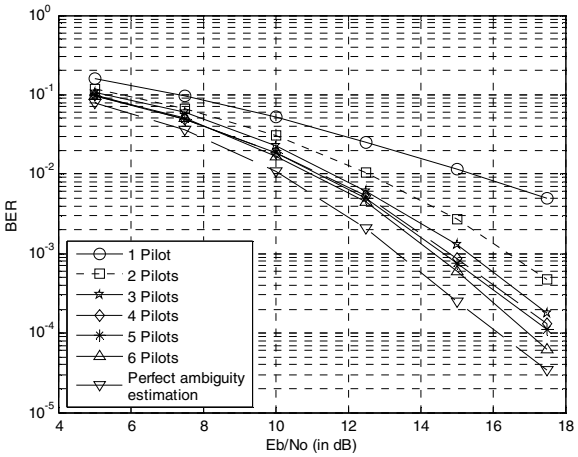

Fig. 3. BER of SC-FDE system employing subspace-based channel estimation for different numbers of pilot symbols used for ambiguity resolution with channel order = 4

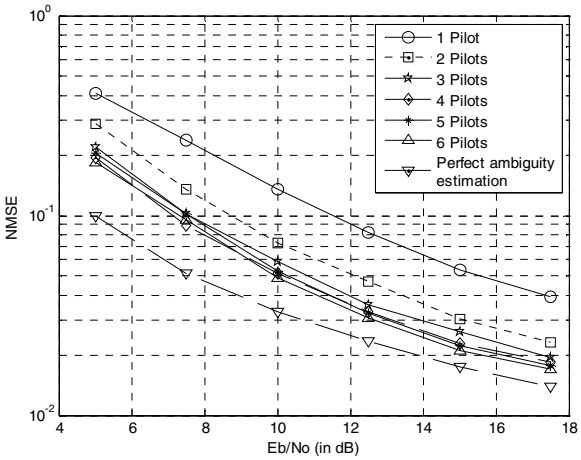

Fig. 4. NMSE of subspace-based channel estimates as a function of $\boldsymbol{E_b/N_o}$ for different numbers of pilot symbols used for ambiguity resolution with channel order = 7

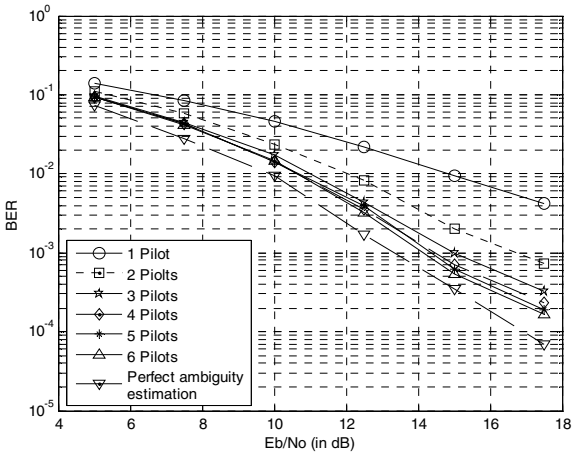

Fig. 5. BER of SC-FDE system employing subspace-based channel estimation for different numbers of pilot symbols used for ambiguity resolution with channel order = 7

References

[1] Ghosh, J. Zhang, J.G. Andrews, R. Muhamed, Fundamentals of LTE, Upper Saddle River, NJ: Prentice Hall, 2011.

[2] 3GPP TS 36.201, "Evolved Universal Terrestrial Radio Access (EUTRA); LTE Physical Layer General Description," Release 12, 2014.

[3] Y. Wang and X. Dong, "Frequency-domain channel estimation for SCFDE in UWB Communications," IEEE Trans. Commun., vol. 54, no. 12, pp. 2155–2163, Dec. 2006.

[4] R. Dinis, C.T. Lam, D.D. Falconer, "Joint frequency domain equalization and channel estimation using superimposed pilots," IEEE Proc. Wireless Commun. and Networking Conf. (WCNC), pp. 447–452, Las Vegas, NV, USA, March 2008.

[5] 3GPP TS 36.211, "Evolved Universal Terrestrial Radio Access (EUTRA); Physical Channels and Modulation," Release 10, 2010.

[6] J.K. Tugnait, L. Tong, Z. Ding, "Single-user channel estimation and equalization," IEEE Signal Proc. Mag., vol. 17, no. 3, pp. 16–28, May 2000.

[7] L. Tong, S. Perreau, "Multichannel blind identification: From subspace to maximum likelihood methods," Proc. IEEE, vol. 86, no. 10, pp. 1951–1968, Oct. 1998.

[8] L. Tong, G. Xu, T. Kailath, "Blind identification and equalization based on second order statistics: a time domain approach," IEEE Trans. Inf. Theory, vol. 40, no. 2, pp. 340–349, Mar. 1994.

[9] S. Haykin, Adaptive Filter Methods, 4th Ed. Upper Saddle River, NJ: Prentice Hall, 2002.

[10] C. D'Amours, B. Champagne, and A.O. Dahmane, "Subspace Decomposition for Channel Estimation in SC-FDE Systems," IEEE Proc. Veh. Tech. Conf. (VTC Spring), pp. 1–5, June 2013.

[11] E. Moulines, P. Duhamel, J.-F. Cardoso, S. Mayrarue, "Subspace methods for the the blind identification of multichannel FIR filters,"IEEE Trans. Sig. Proc., vol. 43, pp. 516-525, February. 1995.